Front. Earth Sci. 2023, 17(1): 58–70
https://doi.org/10.1007/s11707-022-0994-1

RESEARCH ARTICLE

Origin and geological control of desorbed gas in multi-thin coal seam in the Wujiu depression, Hailar Basin, China

Geng LI[1], Yong QIN (✉)[1], Xuejuan SONG[1,2], Boyang WANG[1,3], Haipeng YAO[4], Yabing LIN[1,5]

1 School of Resources and Geosciences, China University of Mining and Technology, Xuzhou 221116, China
2 School of Civil Engineering, Xuzhou University of Technology, Xuzhou 221018, China
3 Institute of Unconventional Oil & Gas, Northeast Petroleum University, Daqing 163318, China
4 Inner Mongolia Autonomous Region Coal Geological Exploration (Group) Co. Ltd., Hohhot 010010, China
5 College of Geology and Environment, Xi'an University of Science and Technology, Xi'an 710054, China

Abstract To understand the natural gas characteristics of multi-thin coal seam, this study selected the desorbed gas of coal seams in different layers of Well A in the Wujiu depression, Hailar Basin in northeast Inner Mongolia. The results show that the heavy hydrocarbon content of desorbed gas increases significantly with the increasing depth. Methane carbon ($\delta^{13}C_1$) and ethane carbon ($\delta^{13}C_2$) isotope values are vertically become heavier downwards, while the $\delta^{13}C_{CO_2}$ values did not change significantly. The kerogen is close to the III–II mixed type with the source rocks mainly deposited in a shore/shallow lake or braided-river delta front, and the gas produced has certain characteristics of oil associated gas. However, the characteristics of oil associated gas produced by the organic formed in the shallow-water environment (braided-river delta plain) are not obvious. The sandstone pore and fracture systems interbedded with multi-thin coal seam are well developed. And it is conducive to the migration of methanogenic micro-organisms to coal seams via groundwater, making it easier to produce biogenic gas under this geological condition. During the burial evolution of coal-bearing strata in the study area, when the burial depth reaches the maximum, there are significant differences in the paleotemperature experienced by different vertical coal seams, caused by a high-paleogeothermal gradient, increasing the $\delta^{13}C_2$ of desorbed gas with increasing depth. The above research indicates that there is less biogenic gas in the multi-thin coal seams with relatively developed mudstone, and the multi-thin coal seams with relatively developed sandstones have obvious biogenic gas characteristics. Therefore, for the exploration and development of biogenic gas in low-rank multi-thin coal seams, it is necessary to give priority to the layer with high sandstone content.

Keywords multi-thin coal seam, origin of coalbed methane, desorbed gas, isotopes, geological control

1 Introduction

Because of the successful development of low-rank coalbed methane (CBM) in the United States, Canada, Australia, and other countries, China's low-rank CBM has attracted extensive attention in the natural gas industry recently (Wang et al., 2009; Li et al., 2021a; Yuan et al., 2022). Micro-organisms and other geological factors may significantly affect the transformation of coal-bearing strata after tectonic uplifting, resulting in multiple characteristics of the generated gases. Studying the origin of CBM is critical to understand the resource distribution of CBM. Researchers have divided the genetic CBM types into biogenic and thermogenic gases, and biogenic gas is subdivided into primary and secondary biogenic gases (Scott and Kaiser., 1994; Kotarba, 2001). Schoell (1980) first proposed the $\delta^{13}C_1$ value of –55‰ as the boundary between biogenic gas and thermogenic gas. Gao et al. (2020) concluded that this value is only an approximate indicator, because the range of $\delta^{13}C_1$ value of biogenic gas can range from –40‰ to –110 ‰. The current $\delta^{13}C_1$ value of –50 ‰ is more reasonable for the boundary between biogenic and thermogenic gases. However, for coalbed methane whose $\delta^{13}C_1$ value is about –50‰, we cannot simply classify the origin of the gas according to the $\delta^{13}C_1$ value, because the $\delta^{13}C_1$ value is largely influenced by the isotopic composition of the original organic matter and the pathway of biological methane production. Therefore, coalbed methane with $\delta^{13}C_1$ values of around –50 ‰

Received February 11, 2021; accepted April 7, 2022

E-mail: yongqin@cumt.edu.cn

needs to be analyzed in combination with other chemical indicators, such as methane hydrogen isotope indicators for differentiation (Gao et al., 2020). The $C_1/(C_1 + C_{2+})$ of biogenic gas is high, whereas that of thermogenic gas is low. However, there are some small differences in the quantified results given by different scholars (Bernard et al., 1987; Whiticar, 1999). The carbon isotopes of CO_2 ($\delta^{13}C_{CO_2}$) associated with biogenic gas are heavier, whereas those in thermogenic gas are lighter (Kotarba, 2001). Based on the understanding of gas compositions and isotopes, researchers have proposed a discrimination template to determine the origin of gas (Schoell, 1983; Whiticar et al., 1986; Dai et al., 2014). The differential changes in the components and isotopes of desorbed gas in coal seams depend on the coal and reservoir condition characteristics, all controlled by geological processes, such as sedimentation, tectonic structure, and hydrology (Li Y et al., 2014; Bao et al., 2016; Li et al., 2017; Zhang et al., 2019; Bannerjee et al., 2021; Wei et al., 2021).

The development of CBM in the Surat Basin is a successful case of low-rank CBM globally (Queensland government, 2021), and its multi-thin coal seam conditions are unique. Previous studies on the origin of CBM in the Surat Basin have proposed that methanogenic microorganisms are critical (Papendick et al., 2011; Tang et al., 2018). From previous statistical data on the Middle Jurassic Wallon Formation in the Surat Basin, the cumulative thickness of its coal seam is 20–37 m (Johnson et al., 2010) and it has more than 100 coal seams (Shields et al., 2017). Coal seams with a single-layer thickness lower than 0.5 m accounted for 44%–57%, coal seams with a thickness of 0.5–1.0 m accounted for 24%–27%, and the sum of the two accounted for more than 70%. CBM production in the Bowen Basin, superimposed in the lower part of the Surat Basin, is considerably lower than Surat Basin (Queensland, 2018), and an important difference between Bowen Basin and Surat Basin is their different gas origins (Boreham et al., 1998; Kinnon et al., 2010). Therefore, researching the origin of CBM and its geological control factors explores the reasons for the availability/formation of different CBM resources.

As an important coal base in China, Erlian–Hailar Basin CBM resources in eastern Inner Mongolia have gradually attracted attention (Wang et al., 2019; Zhang and Chen, 2020; Li et al., 2021b; Li et al., 2022). The geological conditions of the Wujiu depression in the Hailar Basin are similar to those of the Surat Basin in Australia. They have the characteristics of low degree of coalification and multi-thin coal seams. Therefore, we selected the Upper Cretaceous Damoguaihe Formation in the Wujiu depression in the periphery of the Hailar Basin and obtained desorbed gas from different layers of Well A. We analyzed its genetic types and geological control mechanism using gas compositions and isotope tests, combined with other experiments and geological data to enrich the research theory of CBM in multi-thin coal seam.

2 Coal samples and test methods

2.1 Geological characteristics and samples

The Wujiu depression is one of several independent depressions in the periphery of the Hailar Basin group. It is a single-fault dustpan-fault depression basin, and its base mostly comprises Jurassic magmatic rocks, most of which are exposed around the basin (Figs. 1(a) and 1(b)). The exploration data show that the Wujiu depression presents a structural pattern of sinking in the northwest and fault sliding in the southeast, characterized by a slow dip angle in the north and a steep large thickness and dip angle of the layer in the south. The coal-bearing stratum in the Wujiu depression is the Damoguaihe Formation, Early Cretaceous. The coal-bearing strata sedimentary system includes a lake, braided-river delta, braided river, fan delta, and alluvial fan (Li et al., 2019). The vitrinite reflectance (R_o) of coal ranges from 0.4% to 0.7%, characterized by lignite to high-volatile bituminous coal.

According to the data of 32 coal exploration borewells in Moguai block, Damoguaihe Formation contains 22–105 coal layers, with an average of 66 layers. And the cumulative thickness of coal seam is 9.45–61.04 m, averaging 32.4 m. The average thickness of single coal seam is 0.81 m, and the coal seam with thickness less than 0.8 m accounts for 66% of the statistical value.

The Wujiu depression is still in the CBM exploration stage, and the CBM wells are few. In this study, the desorbed gas coal samples and the coal and carbonaceous mudstone samples (adjacent layer of the corresponding coal sample) in the corresponding intervals were collected in Well A for testing. There are four core sections in the well. Figure 1 shows the specific conditions and layer locations. Well A is a sectional coring borewell. After the coal was raised for drilling, we disassembled the coring tube and loaded the blocky coal into a sealed tank. We filled the remaining space with quartz and tightened the tank cover. We dipped the tank into water to evaluate its tightness and collected the desorbed gas using the drainage gas-collection method. To avoid CO_2 in the desorption gas dissolving in water, only the saturated sodium chloride solution was left over the bottle stopper. In order to avoid experimental errors caused by desorption fractionation, the gas collected in the second cylinder (the 200–400 cc gas in the desorption process) was selected for this experimental test.

2.2 Methods

Eight samples of desorbed gas were analyzed using gas chromatography to determine the gas components, and

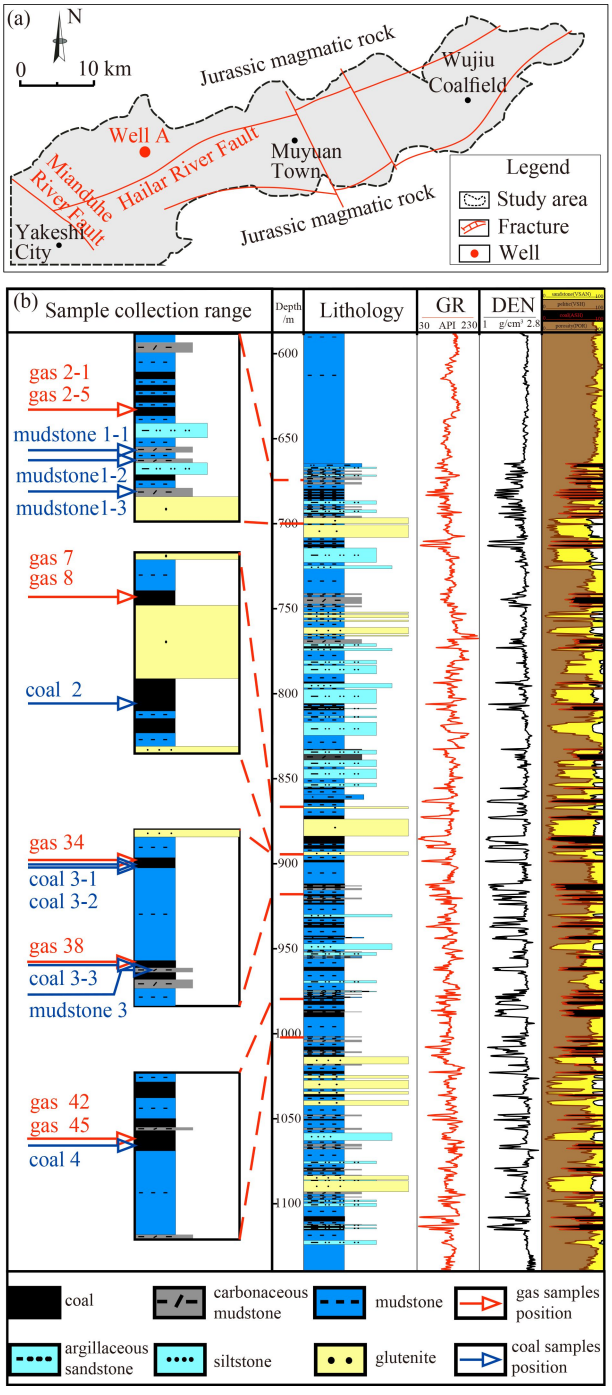

Fig. 1 The structural location of the study area and the drilling columnar of Well A.

carbon and hydrogen isotopes were analyzed. The purpose of the rock pyrolysis analysis of coal and carbonaceous mudstone samples was to understand the type and maturity of organic matter in the corresponding interval. Two desorbed coal samples were selected for elemental analysis in each sampling interval, with a total of eight samples. The reflected light and fluorescence of the coal and rock samples were observed under a Leica electron microscope.

The gas isotope test was completed at the Oil and Gas Resources Research Center of the Northwest Institute of Ecological Environment and Resources, Chinese Academy of Sciences. For the carbon isotope test, the chromatograph model was Trace GC, the chromatographic column model was CP-carbobond, and the isotope mass spectrometer model was MAT253. The measurement accuracy of carbon isotopes was 0.1 ‰–0.5‰. The isotope value is expressed in a $\delta^{13}C$ (V-PDB) form. For the hydrogen isotope test, the chromatograph model was Agilent 7890, the chromatographic column model was Plot Q, and the isotope mass spectrometer model was Isoprime 100. The measurement accuracy of hydrogen isotopes was 1 ‰–2 ‰. The hydrogen isotope value is expressed in δD (V-SMOW).

A gas composition analysis was conducted at Key Laboratory of Coalbed Methane Resources and Reservoir Formation Process, Ministry of Education, China University of Mining and Technology. Au MAT-271 microgas mass spectrometer was used, and each gas sample's concentration was calculated using the correction normalization method. N_2 and O_2 brought in by the ambient air in the gas samples were rejected according to the proportion of N_2/O_2 = 3.73. Finally, a normalization calculation was conducted to obtain the corrected concentration of the eight gas samples.

The rock pyrolysis analysis was completed at the State Key Laboratory of Organic Geochemistry, Guangzhou Institute of Geochemistry, Chinese Academy of Sciences. The selected equipment model was the RockEval-6 Standard pyrolysis analyzer manufactured by French Vinci Technologies.

The low-frequency nuclear magnetic resonance (NMR) experiment uses the MacroMR23-060V large-size NMR analyzer, and one sandstone and one mudstone sample are selected respectively. The experimental steps are as follows. 1) The samples are cut into standard column samples of 2.5 cm × 5 cm by wire cutting instrument. 2) The column samples were dried in a dryer for 24 h at a constant temperature of 50°C. After drying, the samples were weighed and T_2 spectrum test was performed. 3) Put it into the vacuum pressure saturation device to vacuum, then inject water to saturate for 48 hours, set the pressure to 30 MPa, and then take it out for T_2 spectrum test. 4) Centrifugal dehydration, followed by T2 spectrum test. Main NMR test parameters include echo interval time (0.2 ms), waiting time (4 s), echo number (18000), scan number (32) and ambient temperature (22.5°C).

3 Results

3.1 Chemical composition of CBM

The CBM of Well A mostly comprises methane, including some heavy hydrocarbon and nonhydrocarbon

gases. The methane concentration of the hydrocarbon gas accounts for 75.92%–94.37%, averaging 87.96%; its ethane concentration accounts for 0.87%–12.92%, averaging 5.21%; and its propane concentration accounts for 0.10%–5.21%, averaging 1.59%. The nitrogen concentration of the nonhydrocarbon gas accounts for 0%–0.73%, averaging 0.26%; its CO_2 concentration accounts for 1.95%–10.96%, averaging 4.24%. The samples' drying coefficients are 0.79–0.99, averaging 0.92 (Table 1).

Table 1 shows that with the increasing burial depth, the methane concentration decreases, especially in the fourth coring section (985–988 m), and the average methane concentration is only approximately 75%. The ethane and propane concentrations display an increasing trend with the increasing burial depth, and the fourth coring section (985–988 m) is the most obvious. The drying coefficient changes from 0.99 to 0.79, where the thermal maturity is one of its influencing factors. With the increasing burial depth, the heavy hydrocarbon gas component content changes due to thermal causes.

3.2 Carbon/hydrogen isotopic characteristics of CBM

The $\delta^{13}C_1$ ranges from −59.1 ‰ to −49.5 ‰, with an average of −54.6 ‰. The $\delta^{13}C_2$ ranges from −37.4 ‰ to −28.8‰, with an average of −32.3‰. The carbon isotope of propane ($\delta^{13}C_3$) ranges from −33.5‰ to −27.1‰, with an average of −29.5‰ (some samples were not detected). The $\delta^{13}C_1$ and $\delta^{13}C_2$ increased with the increasing depth, but the stable carbon isotope of hydrocarbon gas did not decrease, which is a positive carbon isotope sequence. Combined with the CO_2 stable carbon isotope analysis, the gas sample collected was a typical organic gas (Kotarba, 2001). The carbon isotope composition of CO_2 ($\delta^{13}C_{CO_2}$) ranges from −27.0 ‰ to −24.7 ‰, with an average of −25.6‰. The methane hydrogen isotope (δD) ranges from −307.3 ‰ to −276.2 ‰, with an average of −297.2‰ (Table 2).

The desorbed gas isotopes at different depths differ (Fig. 2). $\delta^{13}C_1$ and $\delta^{13}C_2$ increase with the increasing depth. Propane concentrations are very low in the shallow gas samples, propane carbon isotope is undetected, and the changing trend of $\delta^{13}C_3$ in the deep gas samples is not obvious. The relationship between $\delta^{13}C_{CO_2}$ and the depth is not obvious, and the overall $\delta^{13}C_{CO_2}$ performance is heavier. Statistics of the carbon isotope results of various alkanes are $\delta^{13}C_1 < \delta^{13}C_2 < \delta^{13}C_3$, which is a positive carbon isotope sequence.

3.3 Rock pyrolysis and elemental analysis

The pyrolysis characteristics of coal samples and carbonaceous mudstone samples are similar. The hydrogen index (HI) of coal samples ranges from 246 to 293 (average 271.8), and the Maximum Temperature (T_{max}) ranges from 422°C to 426°C (average 423.6°C). The HI of carbonaceous mudstone samples ranges from 226 to 266 (average 252), and the T_{max} ranges from 420°C to 432°C (average 426°C) (Table 3). The results of elemental analysis show that the atomic ratio of oxygen/carbon (O/C) ranges from 0.09 to 0.16, with an average of 0.12. The atomic ratio of hydrogen/carbon (H/C) ranges from 0.73 to 0.83, with an average of 0.78 (Table 4).

4 Discussion

4.1 Identification basis of biogenic gas

Based on the abovementioned data, the different researchers' identification template, $C_1/(C_2 + C_3) - \delta^{13}C_1$ on the origin of CBM is used to identify the coal seam desorbed gas (Fig. 3) (Whiticar, 1999). The results showed that the mixed gas contained biogenic gas of varying degrees. The primary biogenic gas is not conducive to keep in reserve. Most primary biogenic

Table 1 Chemical compounds of desorbed gas samples from coal of Well A

Gas samples	Depth/m	Chemical composition percentage of gas/%							Drying coefficient
		C_1 a)	C_2 a)	C_3 a)	C_4 a)	CO	CO_2	N_2	$C_1/(C_1–C_4)$ b)
2-1	691.3	91.05	0.87	0.10	0.02	0.18	7.23	0.55	0.99
2-5	691.6	94.37	1.40	0.13	0.04	0.21	3.60	0.25	0.98
7	887.8	90.51	5.14	0.76	0.20	0.46	2.74	0.19	0.94
8	888.1	92.28	3.05	0.53	0.18	0.26	3.50	0.21	0.96
34	912.3	90.59	4.78	0.85	0.18	0.40	3.20	0.00	0.94
38	918.0	89.40	3.18	0.88	0.24	0.15	5.68	0.47	0.95
42	985.9	83.01	6.66	3.05	0.98	0.13	5.77	0.39	0.89
45	988.0	75.92	12.92	5.21	1.53	0.51	3.79	0.12	0.79

Notes: a) C_1, C_2, C_3, and C_4 are methane, ethane, propane, and butane, respectively; b) $C_1/(C_1–C_4)$ = methane content/total organic gas content.

Table 2 Carbon and hydrogen isotope characteristics of desorbed gas samples from Well A

Gas samples	Depth/m	R_o/%	δ^{13}C/‰				δD/‰
			CH_4	C_2H_6	C_3H_8	CO_2	CH_4
2-1	691.3	0.57	−59.1	−37.4	—	−25.6	−276.2
2-5	691.6	0.59	−56.6	−35.4	—	−27.0	−286.4
7	887.8	0.60	−55.9	−33.0	−29.0	−24.7	−302.8
8	888.1	0.60	−54.8	−32.4	−27.9	−24.9	−301.8
34	912.3	0.66	−49.5	−28.8	−27.1	−25.7	−292.6
38	918.0	0.63	−55.6	−32.2	−33.5	−25.9	−303.7
42	985.9	0.69	−53.2	−30.5	−30.2	−25.7	−307.1
45	988.0	0.68	−51.9	−28.9	—	−25.0	−307.3

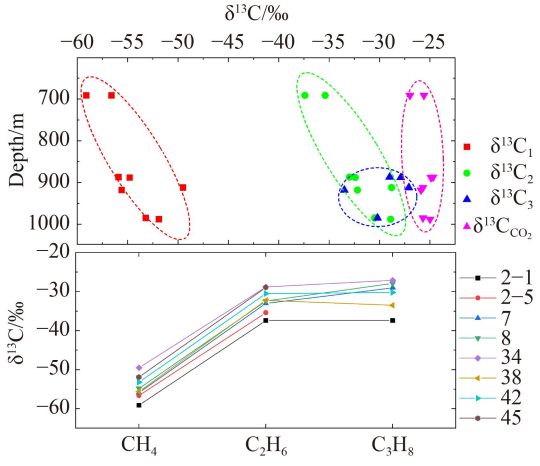

Fig. 2 Variation characteristics of various carbon isotopes in the desorbed gas.

gases will escape when geological conditions (structure and hydrology) changed. For Well A in the study area, the burial history and heating history of the stratum show that in the early stage of deposition that may produce primary biogas, the stratum is buried rapidly, and the ground temperature rapidly exceeded 50°C (Fig. 6). However, the research results of Gao et al. (2020) show that when the local temperature exceeds 50°C, the coal seam will hardly produce biogenic methane. Even if a small amount of early biogenic gas is produced, the early biogenic gas will also escape with the generation and escape of thermogenic gas. In comparison, the geological environment is more favorable for the generation and preservation of secondary biogenic gas after the local stratum is uplifted again. Therefore, the biogenic gas in the present coal seam is mainly secondary biogenic gas. With the increasing burial depth, the secondary biogenic gas content decreases significantly. There are two main reasons for this. 1) It is more difficult for methanogenic microorganisms to decompose organic matter as the metamorphic degree increases (Wang et al., 2018). 2) There could be significant differences in the number of vertical methanogens; that is, there are more methanogenic micro-organisms in the shallow coal seams (600–900 m) but fewer methanogenic microorganisms in the deep coal seams (approximately 1000 and over 1000 m).

4.2 Vertical variation of δ$^{13}C_1$ & δ$^{13}C_2$

The δ$^{13}C_2$ increases as the depth increases (Fig. 2). Biogenic gas hardly produces ethane, eliminating the vertical change in the carbon isotopes caused by biogenic gas. As a typical self-generated and self-storage gas reservoir, CBM exhibits more obvious characteristics in the low-maturity stage. Therefore, the direct factors affecting gas characteristics are mainly organic matter type and maturity (Gao et al., 2020; Bannerjee et al., 2021). With the increasing maturity, hydrocarbon gas δ^{13}C will become heavier to a certain extent (Gao et al., 2020). The metamorphic degree of the coal at 688 and

Table 3 Pyrolysis results of coal and carbonaceous mudstone in the coring section of Well A

Coal samples	Depth/m	HI	T_{max}/°C	Carbonaceous mudstone samples	Depth/m	HI	T_{max}/°C
Coal-2	896.00	287.00	422	CM-1-1	692.95	226.00	432
Coal-3-1	912.44	268.00	426	CM-1-2	693.20	254.00	420
Coal-3-2	912.60	265.00	425	CM-1-3	699.55	266.00	428
Coal-3-3	918.00	246.00	422	CM-3	918.80	262.00	424
Coal-4	987.00	293.00	423				

Notes: Coal-X represents the coal sample of the X-coring section, and CM-X represents the carbonaceous mudstone sample of the X-coring section.

Table 4 Elemental analysis results of coal samples corresponding to desorbed gas of Well A

Coal samples	Depth/m	Maceral composition/%			R_o/%	Element content percentage/%			Atomic ratio	
		V	I	E		O	H	C	O/C	H/C
2-1	691.3	99.0	0.0	1.0	0.57	16.23	5.18	74.79	0.16	0.83
2-5	691.6	98.2	0.0	1.8	0.59	15.72	4.66	75.97	0.16	0.74
7	887.8	/	/	/	0.60	12.02	4.87	80.53	0.11	0.73
8	888.1	/	/	/	0.60	9.73	5.13	82.45	0.09	0.75
34	912.3	98.1	0.7	1.2	0.66	11.88	5.11	80.65	0.11	0.76
38	918.0	99.1	0.0	0.9	0.63	13.75	5.32	77.68	0.13	0.82
42	985.9	97.1	0.0	2.9	0.69	11.19	5.55	80.32	0.10	0.83
45	988.0	94.6	0.9	4.4	0.68	10.26	5.58	81.03	0.09	0.83

Notes: The number of the coal samples used for element testing are consistent with those used for gas isotope testing. V, vitrinite; I, inertinite; E, exinite.

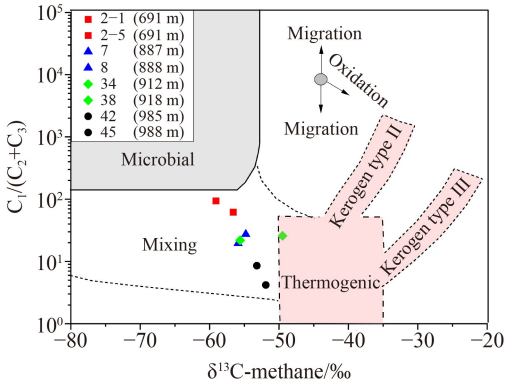

Fig. 3 Template for identifying genetic types of coalbed methane (Template is quoted from Whiticar (1999)).

887–988 m shows the characteristics of a high metamorphic degree in the lower coal seams. Therefore, $\delta^{13}C_2$ become heavier downwards. Furthermore, the organic matter type test shows that with the increasing depth, kerogen-type source rock changes from the III type to III-II mixed type (Fig. 4); it proposes that the characteristics of producing oil associated gas are more obvious. If so, the corresponding $\delta^{13}C_2$ will be lighter as the depth increases, contrary to the actual test results. Therefore, differences in the kerogen types have a negligible effect on the vertical change in $\delta^{13}C_2$. Another cause of heavier isotope values is gas fractionation (Clayton et al., 1997; Chen et al., 2020; Lu et al., 2021). Combined with Table 2, it can be found that the gas samples (2-1 & 2-5, 7 & 8, 42 & 45) in the adjacent layers are light at the top and heavy at the bottom, but the variation range of $\delta^{13}C_1$ and $\delta^{13}C_2$ values is less than 2.5 ‰, indicating that small-scale isotopic fractionation exists in a short distance. Comparing the $\delta^{13}C_1$ and $\delta^{13}C_2$ values from gas samples 2-1 (the highest layer) and 45 (the lowest layer), it can be found that the $\delta^{13}C_1$ and $\delta^{13}C_2$ values have changed 7.2‰ and 8.5‰, respectively, which may be associated with isotope fractionation. However, we carefully observed the changes of δD values in Table 2, and found that the δD value showed a trend of becoming lighter from shallow to deep, with a lighter range of more than 30‰. This phenomenon is contrary to the result of isotope fractionation, so it is considered that gas fractionation is not the main reason that affects the variation of gas isotopes in the vertical whole (buried depth range from 690 to 990 m). Excluding the above two factors, another reason that can lead to vertical change of gas isotopes is thermal maturity of coal. The study shows that the gas isotopes will become heavier with the increase of thermal maturity, which is consistent with the $\delta^{13}C_1$ and $\delta^{13}C_2$ values. Biogenic gas mixing can lead to a heavier δD value of methane because CO_2 reduction can make the δD value of methane heavier than –250 ‰ (Whiticar et al., 1999; Harris et al., 2008). Combined with the analysis results in Setion 4.1, it is believed that with the increase of depth, biogenic gas content will decrease, and the phenomenon of heavier δD value caused by CO_2 reduction will tend to weaken. In conclusion, the $\delta^{13}C_2$ value increases with depth because of the increase of coal maturity, while the $\delta^{13}C_1$ and δD value of methane is the result of the mixing of thermogenic gas and biogenic gas.

4.3 Source of desorbed gas

According to the elemental analysis and rock pyrolysis results, the organic matter types of the coal samples in the desorption and adjacent layers are between type III and the III-II mixed type, which is typically close to the III-II mixed type; that is, the coal in this study is mainly of sapropel humic type (Fig. 4) (Monthioux et al., 1985; Mukhopadhyay et al., 1995; Wang and Zhao, 2020). The vertical span of desorbed gas is approximately 300 m, corresponding to the abovementioned isotopic research results. The greater the depth, the more obvious are the characteristics of the oil associated gas, which is consistent with the rock pyrolysis hydrogen index (HI) analysis trend. With the increasing burial depth, the HI increases. The kerogen type is closer to sapropelic, and its

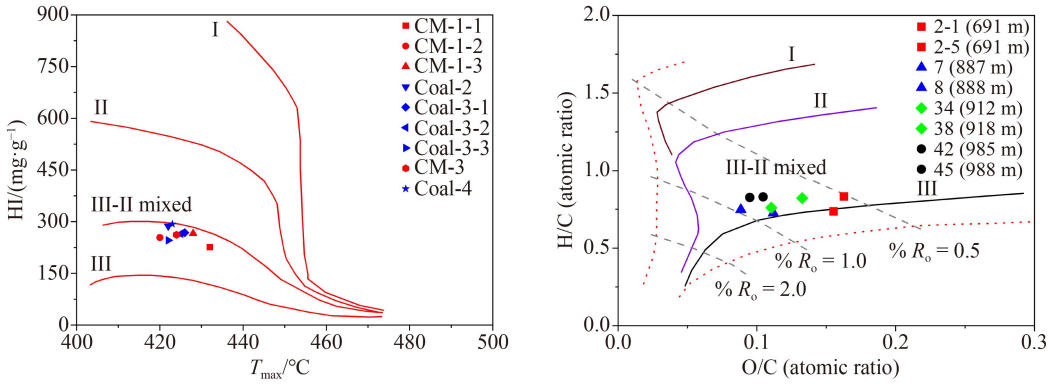

Fig. 4 Identifying kerogen-type source rocks by hydrogen index (HI)-T_{max} and O/C–H/C templates (Mukhopadhyay et al., 1995; Wang and Zhao, 2020).

oil generation capacity is stronger. The O/C–H/C diagram also exhibits this phenomenon, and the source rock reached the oil generation period. The maceral composition results of coal samples Table 4 show that the content of exinite in coal samples is small, but with the increase of depth, the content of exinite tends to increase, indicating that the coal samples are more capable of producing oil and gas. Some lacustrine sediments at the depth of 1000 m in Well A have significant characteristics, which is conducive to the enrichment of organic matter in oil and gas production. Previous studies on Hailar Basin suggest that lacustrine sediments formed during Damoguaihe Formation have good basis for oil and gas generation, and Damoguaihe Formation has oil and gas display in many areas of Hailar Basin (Feng et al., 2004; Wang et al., 2018). The gas logging value of Well A in Fig. 7 shows that C_{2+} heavy hydrocarbon has an obvious increase trend in the deep section below 900 m, which also indicates the objective fact that oil associated gas exists at the depth below 900 m in Well A, and the oil associated gas content increases significantly with the increase of depth. The above evidence shows that the coal seam desorbed gas in Well A (samples 42 & 45) is the comprehensive result of the near-source migration of the gas from organic matter in adjacent layers of sand-mudstone to the reservoir of coal seams and the methane produced by coal itself.

The type of kerogen is a critical for the genetic identification of desorbed gas and is effective for analyzing the desorbed gas's source by inverting the desorbed gas's characteristics and taking the kerogen type as the basis. At least three aspects can be obtained from Fig. 5. 1) Biogenic gas in desorbed gas must exist, and its content is high, which is consistent with the research results in Fig. 3. 2) Oil associated gas also exists, but its gas content is less. The coal seam changes from shallow to deep—the kerogen type changes from type III kerogen phase to type III-II mixed kerogen, and the $\delta^{13}C_2$ become heavier, which is inconsistent with the conventional understanding (Dai et al., 2014). Therefore, the kerogen type has little influence on the desorbed gas' characteristics, whereas other more crucial factors affect the gas' characteristics. 3) There are obvious vertical differences in the thermogenic gas content. With the increasing depth, the degree of metamorphism increases and the methane and ethane isotopes become heavier. From the abovementioned three aspects, the desorbed gas in the shallow coal seam is mainly biogenic gas, followed by thermogenic gas, whereas the gas in the deep coal seam is the opposite. Furthermore, ethane and propane characteristics and identifying kerogen types by rock pyrolysis and elemental analysis show basis for the existence of oil associated gas in desorbed gas. The oil associated gas content also increases with the increasing depth; however, its content is small and its influence on the isotopes of desorbed gas is extremely weak.

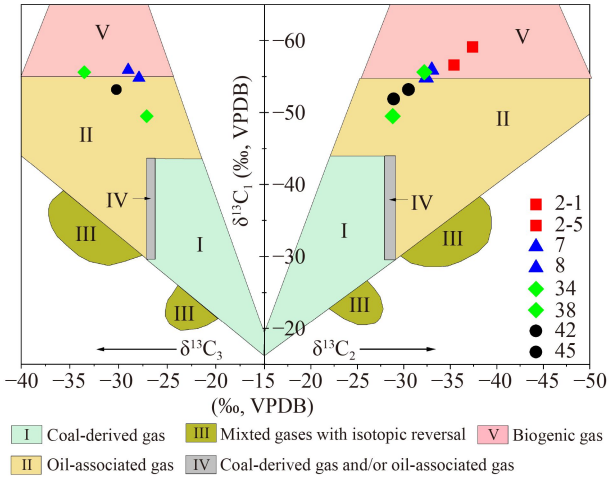

Fig. 5 The $\delta^{13}C_1$–$\delta^{13}C_2$–$\delta^{13}C_3$ plate identifies the genetic type of gas (template is quoted from Dai et al. (2014)).

This study further confirms the understanding of the above three aspects by analyzing the burial–thermal–hydrocarbon generation evolution of coal-bearing strata. Based on the above analysis of the coal measure burial–uplift process and EASY% $R_{o,\,max}$ chemical kinetic model, Shang (2020) conducted a numerical simulation of the burial evolution process (Fig. 6(b)-2) and recovered

the formation temperature change during geological evolution (Fig. 6(b)-1) of Well A in the study area using the PetroMod basin analysis software developed by a German IES company. During the drilling of Well A, a rock fracture zone was encountered at 892–895 m, and many calcite crystals filled the fracture. In this study, calcite in the fracture was selected for inclusion in the homogenization temperature test and 25 test points were selected for each sample. The test results showed that the homogenization temperature of inclusions is 80°C–90°C (Figs. 6(a)-2 and 6(a)-3), whereas the corrected inclusion capture temperature can reach more than 100°C, which has reached the thermogenic gas generation stage (Fig. 6(c)). The coal seam temperature under conditions obtained from well logging is approximately 25°C (Fig. 6(a)-1), which is the appropriate temperature for biogas generation. According to the burial evolution process of Well A and the temperature characteristics, the thermogenic gas in the desorbed gas is mostly formed at the initial burial stage (with high temperatures), whereas at the present stage (with low temperatures), thermogenic gas is not produced (Fig. 6). The vitrinite reflectance test shows that the coal seam exhibits a low metamorphic degree and presents the material basis of biogenic gas production. Therefore, the gas produced by the main coal-bearing strata of Well A under the burial depth and temperature of recent tens of millions of years is mainly biogenic gas (Fig. 6).

4.4 Geological control mechanism of desorbed gas characteristics

Sedimentation, hydrology, and tectonism represent the macroscopic mechanism of geological control. The sedimentation is mainly reflected in the source rock types and lithologic assemblages. The hydrology is reflected in the control action of groundwater dynamic conditions and microbial environment. Tectonism not only affects the metamorphic degree of source rocks but also affects the preservation conditions of gas. The coupling of the above three geological processes caused the existing CBM (Bao et al., 2016; Zhang et al., 2019; Bannerjee et al., 2021; Li et al., 2021a; Wei et al., 2021). Tectonism affects the coal-bearing strata of Well A in the Wujiu depression. The R_o shows that coal maturity had reached the oil generation threshold. The results of the element and rock pyrolysis tests showed that with the increasing depth, oil associated gas characteristics are more obvious in the process of the source rock's kerogen type changing from III to III-II mixed. The gas logging results of Well A

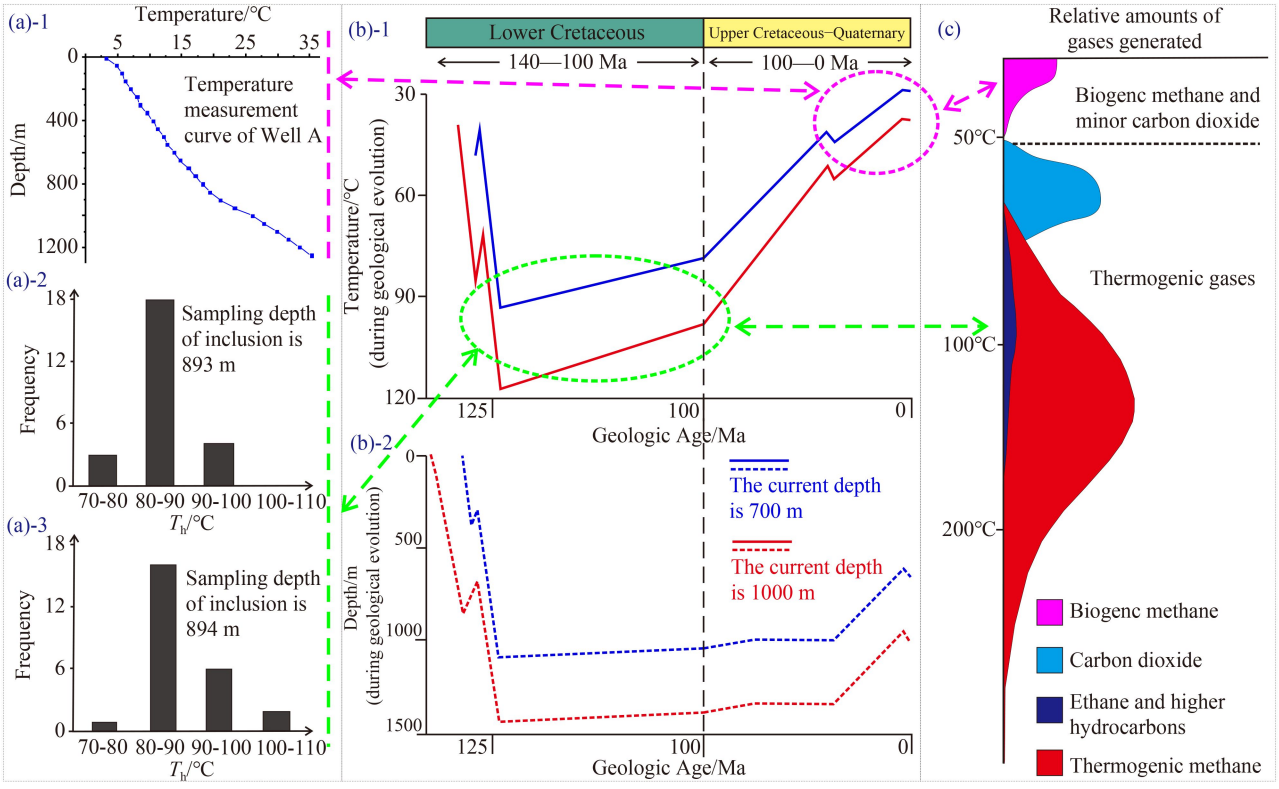

Fig. 6 Relationship between the burial–thermal evolution and hydrocarbon generation characteristics. (a)-1 Vertical variation characteristics of the current formation (Well A) temperature. (a)-2 and (a)-3 Homogenization temperature results of the prescription calcite inclusion test in Well A at 893 m. (b)-1 The relationship between the burial depth and time of Well A. (b)-2 The relationship between the paleotemperature and time of Well A. (c) The characteristics of gases produced at different burial temperatures (the chart is quoted from Gao et al. (2020)).

showed that with the increasing burial depth, the measured value of methane gas decreases significantly, whereas the content of heavy hydrocarbon increases significantly, confirming that the lower part of Well A exhibits oil associated gas characteristics (Fig. 7). From the perspective of the geological control mechanism, the coal-bearing strata in the study area mainly experienced the transition of lake water from deep to shallow and then to deep. The sedimentary facies transformation from the bottom to the top mostly manifests in shore/shallow lake facies, braided-river delta front facies, braided-river delta plain facies, and braided-river delta front facies (Fig. 7). Differences exist in organic matter types in different sedimentary facies. Organic matter in a deep-water environment can provide a material basis for producing oil associated gas. In a shallow-water environment, it forms coal-type gases (Gonçalves et al., 2021; Souza et al., 2021). In the shore/shallow lake facies of Well A, the gas produced by organic matter has the characteristics of oil associated gas. However, in the braided-river delta plain facies, the gas produced by organic matter has no obvious characteristics of oil associated gas. In the braided-river delta front facies, the gas production characteristics of organic matter are between those of the above two gases.

The activity of underground microorganisms mostly controls secondary biogenic gas generation, and the fundamental geological control mechanism is the characteristics of groundwater. Lithologic characteristics mostly control the groundwater flow. The water-bearing characteristics of sandstone are more obvious than that of mudstone, and groundwater flows more easily in sandstone (Figs. 8 (b)-1 and 8(b)-2). Qin et al. (2019) highlighted that the natural fractures formed by thin rock layers are denser than those formed by thick rock layers and that the high-density fracture system is conducive to groundwater activities (Fig. 8(a)-1 and 8(a)-2). According to the statistics of 32 wells, the average thickness of a single mudstone layer of the Damoguaihe Formation is 3.2 m. The average thickness of a single sandstone layer is 4.2 m. The average thickness of a single coal seam is only 0.8 m, of which coal seams with thicknesses of less than 0.8 m account for 66% of the statistical layers. Due to the limitation of logging interpretation accuracy, the above statistical rock stratum thickness is more than 20 cm. Statistics show that the coal-bearing strata of the Damoguaihe Formation of the Upper Cretaceous in the Wujiu depression exhibit a small single-layer thickness and have many rock layers. The groundwater flow is accompanied by methanogenic micro-organism activities. Therefore, in the layers where groundwater is more active, secondary biogenic gas characteristics are more obvious (Fig. 7). Previous studies on microbial methane production under different hydrochemical conditions showed that it decreased with the increase of salinity, so it was considered that low salinity water environment was conducive to methanogenic activities (Su et al., 2011). The pH value in a certain range is conducive to the survival of methanogenic microorganisms. When pH value is greater than 8, the methane production by

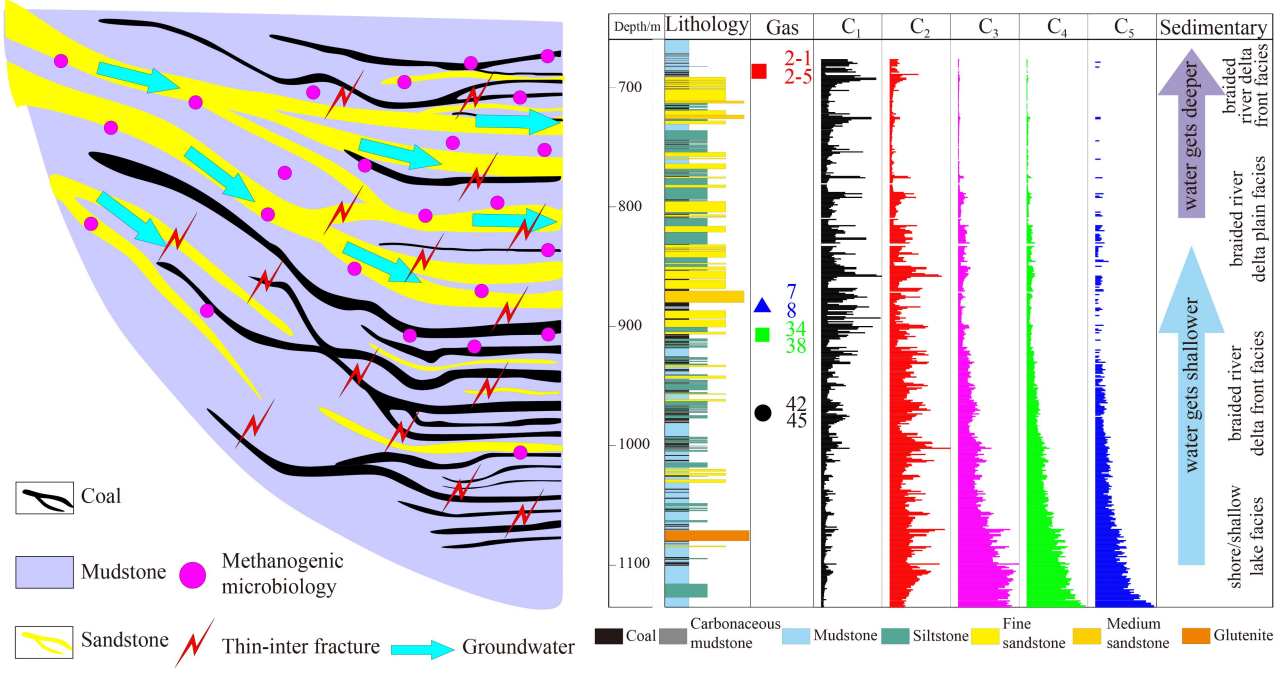

Fig. 7 Geological control mechanism of desorbed gas characteristics of multi coal seams in Well A. C_1, C_2, C_3, C_4, and C_5 in the figure are methane, ethane, propane, butane, and pentane, respectively. The variation range of C_1, C_2, C_3, C_4, and C_5 content are 0–9.2%, 0–0.16%, 0–0.10%, 0–0.05% and 0–0.01%. The above data are from gas logging while drilling.

microorganisms decreases sharply (Hu et al., 2009; Su et al., 2011). The retention degree of ground water also affects the generation of secondary biogenic gas. When the groundwater is in the retention environment, methanogenic microorganisms cannot be transported to coal seam activities, so the formation with too strong sealing is not conducive to the generation of secondary biogenic gas (Tamamura et al., 2019; Zhang et al., 2020). Test results of hydrologic well in coal field adjacent to Well A in the study area is shown in Table 5 (Zhang, 2020). The salinity of each layer is low, which is conducive to the survival of methanogenic bacteria, while the pH value of section-3 (layer section corresponding to gas 42 & 45) is as high as 8.65. Combined with previous research results, it is considered that this stratum is not suitable for microorganisms to produce methane in large quantities. The results showed that the formation water sealing index (F*) of section-3 was higher, while that of section-1 & 2 (layer section corresponding to gas 2-1 & 2-5 and 7 & 8 & 24 & 38) was significantly lower. Therefore, it is considered that section-1 & 2 has strong groundwater activity, which is conducive to the migration of microorganisms by groundwater to the coal seam for methane production. In addition, the above results of formation water sealing are consistent with the control results of formation lithology on groundwater activities, that is, compared with mudstone strata, the groundwater is more active in sandstone strata. Taking the above evidence together, it is confirmed that section-1 & 2 (layer section corresponding to gas 2-1 & 2-5 and 7 & 8 & 24 & 38) is more conducive to the formation of secondary biogas than section-3 (layer section corresponding to gas 42 & 45), which is consistent with the isotope test results. Groundwater activity is beneficial to the generation of secondary biogenic gas, but the strong hydrodynamic conditions may destroy the gas reservoir and make the gas migrate and escape with groundwater, or groundwater activity may also form the hydraulic plugging gas reservoir and make the gas accumulate (Tang et al., 2018). Therefore, whether coal measure gas can be well preserved and enriched in this geological condition still needs a lot of research to confirm.

The increasing coal maturity mostly caused the vertical variation characteristics of the $\delta^{13}C_2$ in Section 3.2. The R_o shows that the metamorphic degree of the coal in the lower part of the coal-bearing strata is significantly higher than that in the upper part. The simulation results of the paleothermal history in the Hailaer Basin show a high

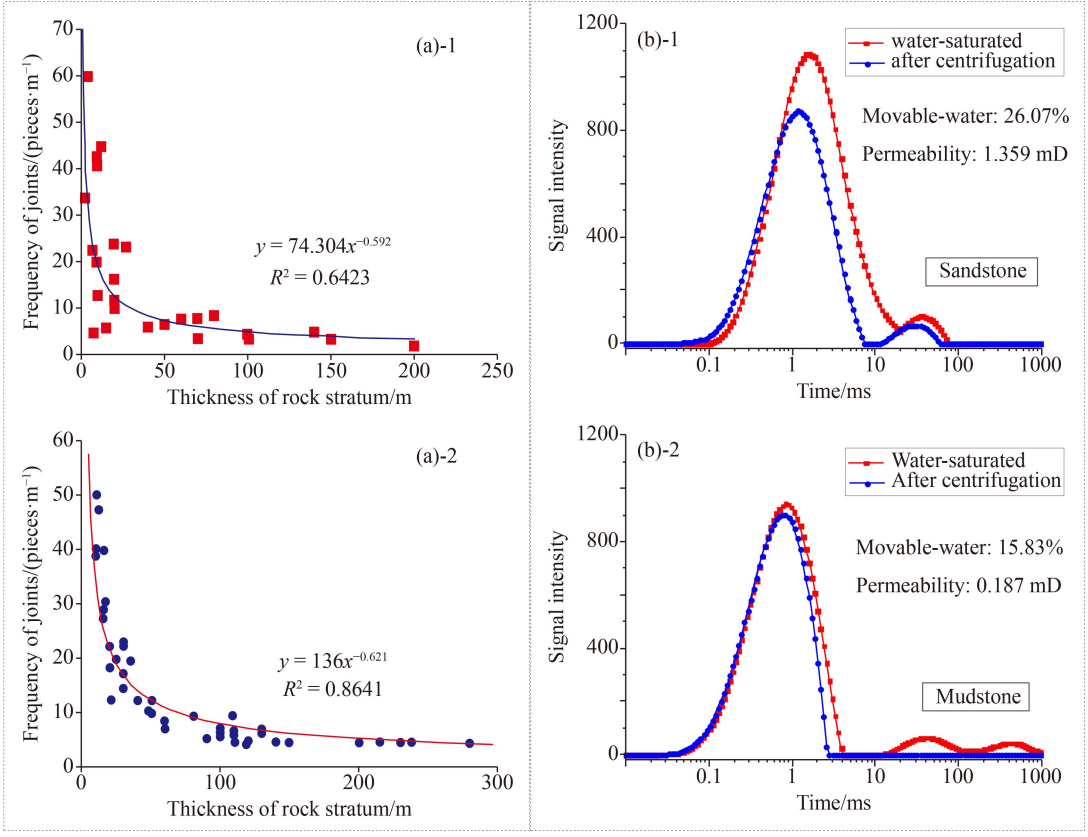

Fig. 8 Characteristics of pores and fissures in coal-bearing strata. (a)-1 Relationship between joint density and thickness of single rock layer in this study area. (a)-2 Relationship between joint density and thickness of single rock layer in an area of Qinshui Basin, China (Qin et al., 2019). (b)-1 NMR results of sandstone sample before and after centrifugation. Sandstone contains more movable water content and higher permeability. (b)-2 NMR results of mudstone sample before and after centrifugation. Mudstone has less movable water content and lower permeability.

Table 5 Calculation results of water sample ion composition and formation sealing

Section	Ion concentration/(mg·L^{-1})								Salinity/(mg·L^{-1})	pH	F*	Sealability
	K^+	Na^+	Ca^{2+}	Mg^{2+}	HCO_3^-	SO_4^{2-}	Cl^-	CO_3^{2-}				
Section-1	9.08	205.98	11.19	4.27	346.79	82.42	44.92	49.94	767.74	/	6.2	Weak
Section-2	1.17	51.63	14.5	3.27	178.17	12.91	8.17	0	290.33	7.8	7.8	Weak
Section-3	1.21	155.56	0.41	2.01	391.33	10.92	8.17	6.26	590.22	8.65	41.7	Stronger

Notes: Data refer to Zhang (2020). Formation sealing (F*) = $\frac{[K^+]+[Na^+]+[HCO_3^-]+[Cl^-]}{[Ca^{2+}]+[Mg^{2+}]+[SO_4^{2-}]}$.

heat flow value in the Damoguaihe Formation. Shang's (2020) study on the thermal evolution history of the study area shows that the paleotemperature of the Damoguaihe Formation reaches a maximum during 126–125 Ma and the paleotemperature range span is extremely large (65°C–130°C). The paleotemperature gradient is as high as 10.43°C/hm, which is much higher than the current geothermal gradient in the study area (3°C/hm). Liu et al. (1994) simulated the paleo-thermal history of Hailaer Basin and found that high terrestrial heat flow value appeared in Damoguaihe period. Tests on calcite inclusions in coal-bearing strata showed that the strata experienced at least 90°C high temperature, and the burial depth was no more than 1300 m (Shang, 2020), so the geothermal gradient at the time of inclusion generation was at least 7°C/hm. Previous research on magmatism in Northeast China shows that there is a large amount of volcanic activity around 125 Ma, which is the maximum burial period of Damoguaihe Formation, and magmatism may be the direct reason for the high geothermal gradient in this period (Wang et al., 2006; Zhang et al., 2008; Li et al., 2014; Su et al., 2021). The higher vertical temperature difference directly affects the maturity and hydrocarbon generation intensity of organic matter. From the top to the bottom, $\delta^{13}C_2$ become heavier as the thermal maturity increases. Shang (2020) proposed that this stage (rapid subsidence and warming, i.e., the stage with a great paleotemperature range) is one of the most critical factors for the current gas-bearing property of coal measures. In conclusion, tectonic sedimentation controls the geological control mechanism of the vertical change in $\delta^{13}C_2$. Obvious differences exist in the paleotemperature experienced by organic matter at different burial depths, resulting in obvious differences in thermal maturity, manifested in that the desorbed gas $\delta^{13}C_2$ of coal seams with large burial depth (high paleotemperature) is heavier, whereas the desorbed gas $\delta^{13}C_2$ of coal seams with shallow burial depth (high paleotemperature) is lighter. Many faulted basins in China were formed in the Jurassic–Cretaceous system, during which volcanic eruptions were frequent. The formation and development of faulted basins often showed that sedimentary basins faults were more active in this period and that the underground magma often affected the evolution of sedimentary organic matter to varying degrees (Su et al., 2021). Therefore, the study of coal and coalbed methane in China's faulted basins cannot be conducted at a single scale. Even in the same depression, obvious differences may exist in the evolution process and properties of coal seams in different layers and positions.

5 Conclusions

From component and isotope tests of desorbed gas, demonstration pyrolysis and element analysis of coal (mudstone), homogenization temperature tests of calcite inclusions, and geological simulations and data analysis, two key conclusions were obtained.

1) The genetic type of desorbed gas from multiple coal seams in Well A is mainly the result of thermogenic gas and secondary biogenic gas mixing. Furthermore, a small amount of oil associated gas is present in Well A.

2) Controlled by sedimentation, the types of deposited organic matter vertically in Well A changed, and the components and isotopes of gas produced by different types of organic matter showed obvious differences. The pore-fracture system of multi-thin coal seam with developed sandstone is conducive to the activities of methanogenic microorganisms carried by groundwater, which is more likely to produce secondary biogenic gas. Controlled by tectonic, the maximum paleotemperature differences in coal seams at different depths of Well A are obvious, affecting the characteristics of gas produced in different coal seams, manifested as the vertical change in $\delta^{13}C_2$.

Acknowledgements We would like to thank the National Natural Science Foundation of China (Grant Nos. 42130802, 42002193, and 42002186) and researchers Yanqiu Zhang, Wutao Hu, Haitao Lin, and Fengchun Li from Inner Mongolia Coal Geology Bureau for their help in sample acquisition. Thank anonymous reviewers for their valuable suggestions. Furthermore, we would like to thank Master Zhen Zhang from China University of Mining and Technology for his help in field work.

References

Bannerjee M, Mendhe V A, Kamble A D, Varma A K, Singh B D, Kumar S (2021). Facets of coalbed methane reservoir in East Bokaro Basin, India. J Petrol Sci Eng, 208: 109255

Bao Y, Wei C, Neupane B (2016). Generation and accumulation characteristics of mixed coalbed methane controlled by tectonic evolution in Liulin CBM field, eastern Ordos Basin, China. J Nat Gas Sci Eng, 28: 262–270

Bernard B B, Brooks J M, Sackett W M (1978). Light hydrocarbons in recent Texas continental shelf and slope sediments. J Geophys Res, 83(C8): 4053–4061

Boreham C J, Golding S D, Glikson M (1998). Factors controlling the origin of gas in Australian Bowen Basin coals. Org Geochem, 29(1–3): 347–362

Chen Y, Zhang B, Qin Y, Li Z, Yang Z, Wu C, Cao C (2020). Differences in CH_4 and C_2H_6 carbon isotopic compositions from open and closed pores in coal: implications for understanding the two-stage $\delta^{13}C$ shift during canister desorption. Int J Coal Geol, 230: 103586

Clayton C J, Hay S J, Baylis S A, Dipper B (1997). Alteration of natural gas during leakage from a North Sea salt diapir field. Mar Geol, 137(1–2): 69–80

Dai J, Gong D, Ni Y, Huang S, Wu W (2014). Stable carbon isotopes of coal-derived gases sourced from the Mesozoic coal measures in China. Org Geochem, 74: 123–142

Feng Z, Ren Y, Zhang X, Zhang J, Dong W, Li C, Li F (2004). Law of oil gas distribution in Hailar Basin and orientation for exploration at next stage. China Petrol Explor, 4: 19–22+1 (in Chinese)

Gao L, Mastalerz M, Schimmelmann A (2020). The origin of coalbed methane. In: Thakur P, Schatzel S J, Aminian K, Rodvelt G, Mosser, M M, D'Amico, J S, eds. Coal Bed Methane (2nd ed), Elsevier: 3–34

Gonçalves P A, Morgado A, Filho J G M, Mendonça J O, Flores D (2021). Paleoenvironmental variations in a sedimentary Jurassic sequence from Lusitanian Basin (Portugal). Intern J Coal Geo, 247: 103858

Harris S H, Smith R L, Barker C E (2008). Microbial and chemical factors influencing methane production in laboratory incubations of low-rank subsurface coals. Intern J Coal Geo, 76(s1–2): 46–51

Hu Y, Yuan Y, Yan Z, Liao Y, Liu X, He R, Zhang H, Guan J (2009). Isolation and phylogenetic analysis of a methanogen with wide growth pH range. Chin J Appl Environ Biol, 15(04): 554–558 (in Chinese)

Johnson R L, Scott M P, Jeffrey R G (2010). Evaluating hydraulic fracture effectiveness in a coal seam gas reservoir from surface tiltmeter and microseismic monitoring. J Pet Technol, 63(03): 59–62

Kinnon E C P, Golding S D, Boreham C J, Baublys K A, Esterle J S (2010). Stable isotope and water quality analysis of coal bed methane production waters and gases from the Bowen Basin, Australia. Int J Coal Geol, 82(3–4): 219–231

Kotarba M J (2001). Composition and origin of coalbed gases in the Upper Silesian and Lublin basins, Poland. Org Geochem, 32(1): 163–180

Li J, Shao L, Sun B (2019). Sequence-palaeogeography and coal accumulation of the Damoguaihe Formation in the Wujiu mining area, Yakeshi Coalfield, Hailar Basin. J China Coal Soc, 44(S2): 610–619 (in Chinese)

Li G, Qin Y, Yao Z, Hu W (2021a). Differentiation of carbon isotope composition and stratabound mechanism of gas desorption in shallow-buried low-rank multiple coal seams: case study of Well DE-A, Northeast Inner Mongolia. Nat Resour Res, 30(2): 1511–1526

Li G, Qin Y, Zhou X, Zhang Y, Hu W (2021b). Comparative analysis of the pore structure of fusain in lignite and high-volatile bituminous coal. J Nat Gas Sci Eng, 90: 103955

Li G, Qin Y, Zhang M, Wang B, Li J (2022). Microporous structure and gas adsorption model of fusain in lignite. Fuel, 309: 122186

Li S, Hegner E, Yang Y, Wu J, Chen F (2014). Age constraints on late Mesozoic lithospheric extension and origin of bimodal volcanic rocks from the Hailar basin, NE China. Lithos, 190–191: 204–219

Li Y, Tang D, Fang Y, Xu H, Meng Y (2014). Distribution of stable carbon isotope in coalbed methane from the east margin of Ordos Basin. Sci China Earth Sci, 57(8): 1741–1748

Li Y, Zhang C, Tang D, Gan Q, Niu X, Wang K, Shen R (2017). Coal pore size distributions controlled by the coalification process: an experimental study of coals from the Junggar, Ordos and Qinshui Basins in China. Fuel, 206: 352–363

Liu J, Shi G, Guo Q (1994). Quantitative method of recovering thermal evolution history with apatite fission track. Petrol Explor Dev, 04: 15–18+116 (in Chinese)

Lu S, Feng G, Shao M, Li J, Xue H, Wang M, Chen F, Li W, Pang X (2021). Kinetics and fractionation of hydrogen isotopes during gas formation from representative functional groups. Petrol Sci, 18(4): 1021–1032

Monthioux M, Landais P, Monin J C (1985). Comparison between natural and artificial maturation series of humic coals from the Mahakam delta. Indonesia, 8(4): 0–292

Mukhopadhyay P K, Wade J A, Kruge M A (1995). Organic facies and maturation of Jurassic/Cretaceous rocks, and possible oil-source rock correlation based on pyrolysis of asphaltenes, Scotian Basin, Canada. Org Geochem, 22(1): 85–104

Papendick S L, Downs K R, Vo K D, Hamilton S K, Dawson G K W, Golding S D, Gilcrease P C (2011). Biogenic methane potential for Surat Basin, Queensland coal seams. Int J Coal Geol, 88(2–3): 123–134

Qin Y, Shen J, Shen Y, Li G, Fan B, Yao H (2019). Geological causes and inspirations for high production of coal measure gas in Surat Basin. Acta Petrol Sin, 40(10): 1147–1157 (in Chinese)

Queensland Government (2021) Production and reserve statistics. Available at Queensland Government website

Schoell M (1980). The hydrogen and carbon isotopic composition of methane from natural gases of various origins. Geochim Cosmochim Acta, 44(5): 649–661

Schoell M (1983). Genetic characterization of natural gases. AAPG Bull, 67: 2225–2238

Scott A R, Kaiser W R (1994). Thermogenic and Secondary biogenic gases, San Juan Basin, Colorado and New Mexico-Implications for Coalbed Gas Producibility. AAPG Bull, 78(8): 1186–1209

Shang N (2020). Coalification and structural control of Damoguaihe Formation in Wujiu Depression, Inner Mongolia, China. Dissertation for the Doctoral Degree. Xuzhou: China University of Mining and Technology (in Chinese)

Shields D, Bianchi V, Esterle J (2017). A seismic investigation into the

geometry and controls upon alluvial architecture in the Walloon Subgroup, Surat Basin, Queensland. Aust J Earth Sci, 64(4): 455–469

Souza I M S, Cerqueira J R, Garcia K S, Ribeiro H J P S, Oliveira O M C, Queiroz A F S, Teixeira L S G (2021). Geochemical characterization and origin of kerogens from source-rock of Devonian in the Amazonas Basin, Brazil. J S Am Earth Sci, 111: 103437

Su N, Zhu G, Wu X, Yin H, Lu Y, Zhang S (2021). Back-arc tectonic tempos: records from Jurassic–Cretaceous basins in the eastern North China Craton. Gondwana Res, 90: 241–257

Su X, Xu Y, Wu Y, Xia D, Chen X (2011). Effect of salinity and pH on biogenic methane production of low-rank coal. J China Coal Soc, 36(08): 1302–1306 (in Chinese)

Tamamura S, Murakami T, Aramaki N, Ueno A, Tamazawa S, Badrul A, Haq S, Igarashi T, Aoyama H, Yamaguchi S, Kaneko K (2019). The role of meteoric water recharge in stimulating biogenic methane generation: a case study from the Tempoku Coal Field, Japan. Int J Coal Geol, 202: 14–26

Tang Y, Gu F, Wu X, Ye H, Yu Y, Zhong M (2018). Coalbed methane accumulation conditions and enrichment models of Walloon Coal measure in the Surat Basin, Australia. Nat Gas Indust B, 5(3): 235–244

Wang A, Shao P, Lan F, Jin H (2018). Organic chemicals in coal available to microbes to produce biogenic coalbed methane: a review of current knowledge. J Nat Gas Sci Eng, 60: 40–48

Wang B, Li J, Zhang Y, Wang H, Liu H, Li G, Ma J (2009). Geological characteristics of low rank coalbed methane, China. Pet Explor Dev, 36(1): 30–34

Wang B, Qin Y, Shen J, Wang G, Zhang Q, Liu M (2019). Experimental study on water sensitivity and salt sensitivity of lignite reservoir under different Ph. J Petrol Sci Eng, 172: 1202–1214

Wang F, Zhou X, Zhang L, Ying J, Zhang Y, Wu F, Zhu R (2006). Late Mesozoic volcanism in the Great Xing'an Range (NE China): timing and implications for the dynamic setting of NE Asia. Earth Planet Sci Lett, 251(1–2): 179–198

Wang X, Zhao Y (2020). The time-temperature-maturity relationship: A chemical kinetic model of kerogen evolution based on a developed molecule-maturity index. Fuel, 278: 118264

Wang Y, Zhang F, Zou Y, Sun J, Lin X, Liang T (2018). Oil source and charge in the Wuerxun Depression, Hailar Basin, northeast China: a chemometric study. Mar Pet Geol, 89(3): 665–686

Wei Q, Hu B, Li X, Feng S, Xu H, Zheng K, Liu H (2021). Implications of geological conditions on gas content and geochemistry of deep coalbed methane reservoirs from the Panji Deep Area in the Huainan Coalfield, China. J Nat Gas Sci Eng, 85: 103712

Whiticar M J, Faber E, Schoell M (1986). Biogenic methane formation in marine and freshwater environments: CO_2 reduction vs. acetate fermentation—isotope evidence. Geochim Cosmochim Acta, 50(5): 693–709

Whiticar M J (1999). Carbon and hydrogen isotope systematics of bacterial formation and oxidation of methane. Chem Geol, 161(1–3): 291–314

Yuan M, Lyu S, Wang W, Xu F, Yan X (2022). Macrolithotype controls on natural fracture characteristics of ultra-thick lignite in Erlian Basin, China: implication for favorable coalbed methane reservoirs. J Petrol Sci Eng, 208: 109598

Zhang B, Chen Y (2020). Particle size effect on pore structure characteristics of lignite determined via low-temperature nitrogen adsorption. J Nat Gas Sci Eng, 84: 103633

Zhang J (2020). Hydrogeological conditions of controlling gas in coal measures in Wujiu Depression. Dissertation for the Doctoral Degree. Xuzhou: China University of Mining and Technology (in Chinese)

Zhang S, Zhang X, Li G, Liu X, Zhang P (2019). Distribution characteristics and geochemistry mechanisms of carbon isotope of coalbed methane in central-southern Qinshui basin, China. Fuel, 244: 1–12

Zhang Y, Li S, Tang D, Zhao X, Zhu S, Ye J (2020). Structure- and hydrology-controlled isotopic coupling and heterogeneity of coalbed gases and co-produced water in the Yanchuannan block, southeastern Ordos Basin. Int J Coal Geol, 232: 103626